Quantification of VEGF Induced Permeability Changes by Multispectral Analysis

L. R. Berry[1], K. Barck[1], D. Dugger[2], S. P. Williams[1], N. Van Bruggen[1], M. Ostland[3], H. Koeppen[4], R. H. Schwall[2], R. A. Carano[1]

[1]Physiology, Genentech, Inc., South San Francisco, CA, United States, [2]Molecular Oncology, Genentech, Inc., South San Francisco, CA, United States, [3]Biostatistics, Genentech, Inc., South San Francisco, CA, United States, [4]Pathology, Genentech, Inc., South San Francisco, CA, United States

Introduction: Tumor heterogeneity complicates the quantification of a therapeutic response by MRI and further complicates permeability measurements where tumors are often treated as a whole entity, although they often include areas of necrosis and neighboring healthy tissue. Previously, multispectral (MS) analysis was employed to identify and quantify tissue classes within the tumor as a means to address tumor heterogeneity [1]. In this study, the MS analysis technique has been expanded to include measures of microvascular permeability (K^{PS}) and fractional plasma volume (fPV) as a means to extract regions of varying permeability within the viable tumor tissue. First, k-means (KM) clustering was applied to differentiate regions of viable tumor tissue from necrosis and subcutaneous adipose tissue based on apparent diffusion coefficient (ADC), T_2, and proton density (M_0) data for the tumor. Second, the KM clustering algorithm was applied to segment the viable tumor tissue based solely on K^{PS} and fPV into four sub-classes. The ability of this MS permeability technique to detect a change in permeability was evaluated by monitoring the response of two tumor cell lines in vivo to vascular endothelial growth factor (VEGF) administration, a potent permeability and angiogensis stimulus [2].

Methods: The Genentech, Inc. AAALAC accredited review board approved all animal procedures. Human prostate cancer cells (PC3) or Her2 overexpressing cells (Founder 5) at 5×10^6, were implanted subcutaneous in the flank of female athymic nude mice (n = 3 for each cell line) (Charles River Lab, Wilmington, MA). Tumor volumes ranged from 150mm^3 to 500mm^3 (0.5 x length x width^2). This study involves the administration of gadolinium-bovine serum albumin (Gd-BSA) as a contrast agent (3 µl per g body wt. of 100 mg/ml solution) via a jugular catheter. Mice were imaged on day 0 and day 1. On day 1, mice were injected with 10µl of liquid VEGF at a concentration of 100ng/10µl (0.0033mg/kg) subcutaneously inferior to the tumor 30 min prior to imaging.

MR experiments were performed with a Varian 4.7T Unity Inova MR imaging system (Varian Inc., Palo Alto, CA), with a 30 mm quadrature birdcage coil (Morris Instruments, Ottawa, ON). A multislice, diffusion-weighted stimulated-echo imaging sequence was employed to estimate the apparent diffusion coefficient (ADC) on a pixel-by-pixel basis (b-value range: 85 - 1065 s/mm^2, TR = 3 s, TE = 5.5 ms, TM = 200 ms, NEX = 2, δ = 1 ms, and Δ = 203 ms). T_2 maps were constructed from four T_2-weighted images (TE = 4, 25, 46, 67 ms; TR = 3 s, NEX = 2) obtained with a multislice, spin-echo imaging sequence. Diffusion and T_2 data consisted of 12 contiguous, coronal 1-mm-thick slices (FOV = 25.6 x 25.6 mm and a 64 x 64 matrix).

Pre and post contrast R_1 maps were obtained by a variable flip angle 3D gradient echo technique [3]. Pre-contrast 3D gradient echo (3DGE) data sets (TR = 37.5 ms, TE = 1.8 ms, NEX = 2) were acquired at two flip angles (10° and 30°). This data was collected for two FOV's (FOV = 25.6 x 25.6 x 32 mm and a 64 x 64 x 32 matrix), one encompassing the liver (hepatic portal vein for plasma concentration) and the other containing the tumor. After Gd-BSA administration, 30° 3DGE images were acquired every 3.2 minutes, alternating FOV's, for a total of 8 data sets for each FOV. The change in R_1 was used to determine the fPV and K^{PS} for the tumor [4].

MS Analysis: The KM is an iterative clustering algorithm that segments the data into groups of similar pixels based on a distance measure [4]. The KM clustering algorithm (k = 4) segmented the MS data set (M_0, ADC, T_2) into four tissue classes: viable tumor tissue, tumor necrosis 1 (high ADC, short T_2), tumor necrosis 2 (high ADC, long T_2), and adipose tissue. KM was then applied to divide the viable tissue class into four sub-classes based solely on K^{PS} and fPV data: regions of 1) low K^{PS} and low fPV; 2) high K^{PS} and low fPV; 3) low K^{PS} and high fPV; and 4) high K^{PS} and high fPV. All animal data sets were clustered together.

Results and Discussion: The KM algorithm was applied to divide the data into 4 tissue classes and again to divide the viable tumor tissue into 4 permeability classes (Fig. 1). Using this classification method, the addition of exogenous VEGF induced a significant decrease in the fraction of viable tissue that belongs to the low K^{PS} and high fPV class (day 0: 18.7%, post-VEGF: 8.0%, p=0.02) for the PC3 tumor line and trends towards an increase in areas of high K^{PS} and low fPV (p=0.11) for the PC3 tumors. (Fig 2). Founder 5 tumors showed similar trends to the PC3 tumors, but were not significant. P-values were adjusted using the Holm step-down algorithm to adjust for multiple comparisons in the same data set.

This study has demonstrated that a MS approach can quantify distinct regions of permeability and fractional plasma volume of viable tumor tissue in a xenograft mouse tumor model. MS analysis provides a formal method to employ multiple MR parameters for tissue permeability characterization, which can greatly aid the monitoring of tumor response to potential anti-angiogenic therapies.
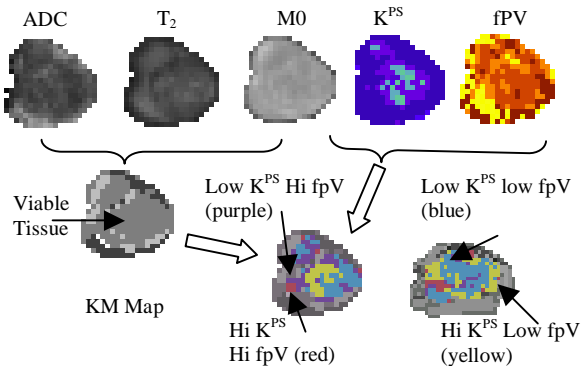

Figure 1: MS K-means classification of tumor tissues. Bottom Row: Pre-VEGF (left) and Post-VEGF (right) permeability (color) and tissue (black and white) class maps.
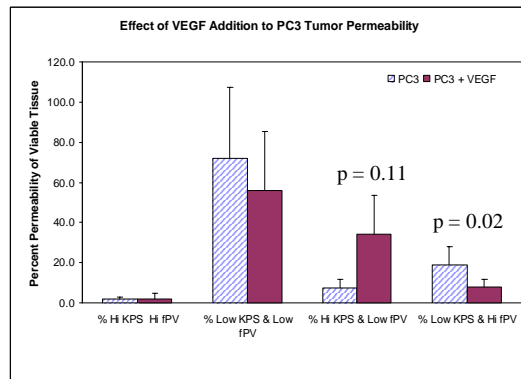

Figure 2: Comparison of pre-VEGF to post-VEGF permeability in PC3 xenograft tumors.

References:
1. Carano RAD, et al., *Magn Reson Med* (in press).
2. Pham CD, et al., *Cancer Invest* **16(4)**, 225-30, 1998.
3. Brookes JA, et al., *Brit J Radiol* **69**, 206-14, 1996.
4. Shames DM, et al., *Magn Reson Med* **29**, 616-22, 1993.